引用格式：ZHANG Wenlin, LIU Kun, JIANG Junfeng, et al. Tungsten Disulfide Modified Tapered Fiber Optic Surface Plasmon Resonance Sensor with Enhanced Sensitivity[J]. Acta Photonica Sinica, 2022, 51(3):0306002
张文林,刘琨,江俊峰,等.基于二硫化钨增敏的锥形光纤表面等离子体共振传感器[J].光子学报,2022,51(3):0306002

基于二硫化钨增敏的锥形光纤表面等离子体共振传感器

张文林,刘琨,江俊峰,徐天华,王双,张炤,井建迎,马金英,刘铁根
(天津大学 精密仪器与光电子工程学院 光电信息技术教育部重点实验室,天津 300072)

摘　要:提出了一种具有增强灵敏度的锥形光纤二硫化钨(WS_2)-金(Au)表面等离子体共振(SPR)传感器。通过传输矩阵方法对传感器进行了理论模拟,评估了传感器的可行性。在锥形光纤上依次涂覆WS_2和溅射金膜进行传感实验,该传感器的实验折射率灵敏度可达4 158.171 nm/RIU,比多模光纤SPR传感器提高了125.8%,比锥形光纤Au-WS_2SPR传感器提高了50.1%。此外,该传感器中的WS_2不易脱落,表现出良好的可靠性。该传感器结构简单、易于制造,具有高的折射率灵敏度,在生化传感领域具有良好的应用前景。

关键词:表面等离子体共振;锥形光纤;灵敏度;二硫化钨;传感器
中图分类号:TN29　　**文献标识码**:A　　**doi**:10.3788/gzxb20225103.0306002

0 Introduction

Fiber optic Surface Plasmon Resonance (SPR) sensors are rapidly becoming key devices in the fields of biological detection, environmental monitoring and food safety due to their superior performance of high sensitivity, anti-electromagnetic interference, label-free, remote monitoring etc.[1-3]. Fiber optic SPR is a phenomenon in which the evanescent field at the surface of the fiber and the surface plasma wave of the metal are coupled and the energy at a certain wavelength will be strongly absorbed. When the external environment changes, the resonance wavelength will move correspondingly[4]. Therefore, biomolecule detection and chemical analysis can be carried out without labels by detecting wavelength changes only.

However, traditional multimode fiber optic SPR sensors are limited by low sensitivity, which leads to their insufficient performance in the detection of low-concentration analytes and small molecular weight biomolecules[5]. Different methods have been studied to overcome this limitation. Among them, it is widely used to improve the sensitivity of sensors by changing the structure of optical fibers (e.g. D-shaped fiber, U-shaped fiber, photonic crystal fiber, hollow core fiber, tapered fiber). Verma theoretically predicted the effect of the tapered fiber on the sensitivity of sensors[6-7]. VIVEK S et al.[8] evaluated the effect of different tapering ratios of tapered fibers on SPR sensors experimentally. The larger the tapering ratio is, the higher the sensitivity is.

Recently, there has been increasing interests in optimizing film structures of fiber optic SPR sensors. The strong electric field excited by the local SPR of metal nanoparticles[9] (e.g. Au, Ag) is used to amplify the SPR

Foundation item: National Natural Science Foundation of China (Nos. 61735011, 61775161, 61922061), Tianjin Science Found for Distinguished Young Scholars (No. 19JCJQJC61400), Ministry of Science and Technology of the People's Republic of China (No. 2013YQ030915)
First author: ZHANG Wenlin (1997—), male, M.S. degree candidate, mainly focuses on surface plasma resonance fiber sensing. Email: 2019202006@tju.edu.cn
Supervisor (Contact author): LIU Kun (1981—), male, professor, Ph.D. degree, mainly focuses on the development of physics and chemistry sensing systems based on optical fiber lasers. Email: beiyangkl@tju.edu.cn
Received: Sep.9,2021; **Accepted**: Oct.19,2021

signal. The modification of one or more dielectric layers (e. g. high Refractive Index (RI) oxides, ceramic materials, two-dimensional materials) on the surface of the metal layer can also be applied to improve the sensitivity. With the discovery of unique optoelectronic properties, graphene has been widely used in the fiber optic SPR sensing due to its unique optoelectronic properties[10-12]. Similar to graphene, Transition Metal Dichalcogenides (TMDCs) have also attracted much attention. Among them, WS_2 shows many unique optoelectronic properties such as high complex RI ratio (the ratio of the real part to the imaginary part of the RI), direct band gap and large surface-to-volume ratio. WU L M et al discussed the enhancement effect of two-dimensional materials on SPR[13]. OUYANG Q L et al[14] theoretically designed a gold-Si-WS_2 heterostructure SPR biosensor to improve the sensitivity of the sensor. A WS_2 nanosheet-assisted prism SPR sensor was reported, and the sensitization effect of WS_2 on the SPR sensor was experimentally proved[15]. However, in aforementioned research works, TMDCs are usually coated by means of the physical adsorption, and they can easily fall off in long-term or repeated use. This will degrade the performance of the sensor[16].

This study aims to contribute to this growing area of SPR research by exploring the impact of WS_2 on tapered fiber SPR sensors. A method for enhancing the sensitivity of SPR sensors is proposed. At first, WS_2 and Au films are sequentially coated on the tapered fiber surface to form the fiber optic SPR sensor. In order to explore the enhancement effect of WS_2, the sensitivities of tapered fiber SPR sensor and tapered fiber WS_2-Au SPR sensor are compared via theoretical simulations and experimental tests. The influence of thicknesses in the WS_2 overlayer on the sensor is discussed. Then, the experimental sensitivity of the sensors with two different structures (Au-WS_2 and WS_2-Au) at the optimal number of coating layers of WS_2 is analyzed respectively. Compared to traditional multimode fiber optic SPR sensors, the sensitivity has been improved. To the best of our knowledge, there are few reported experimental studies on WS_2-assisted fiber optic SPR sensors. Our results show that the tapered fiber WS_2-Au SPR sensor proposed in this paper can significantly increase the sensitivity. Moreover, this structure is simple to manufacture and can provide better reliability.

1 Sensing principles and simulation analyses

1.1 Structure of the tapered fiber WS_2-Au SPR sensor

The proposed tapered fiber WS_2-Au SPR sensor consists of four layers, followed by fiber core, WS_2 layer, metal layer and analyte. The structure of the sensor is schematically illustrated in Fig. 1. The tapering ratio of fiber is defined as: r_i / r_o. $2r_o$ is the minimum diameter of the tapered fiber and $2r_i$ is the initial diameter of the multimode fiber. The length of the sensing area is set as 1 cm[17] and the material of the metal layer is selected as gold and the thickness of the gold film is set as 50 nm, because the 50 nm gold film can provide good resonance response and gold has better stability compared to the silver film[18].

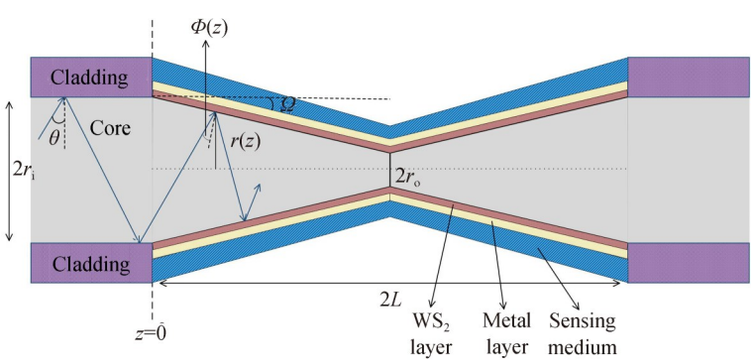

Fig. 1 The schematic configuration of tapered fiber SPR sensor

1.2 Theoretical model of fiber optic SPR sensor

The wavelength-dependent dielectric constant of the fiber core and gold can be expressed by the Sellmeier dispersion relationship and the Drude model, respectively[19]. The relationship between the dielectric constant of WS_2 and the wavelength is obtained by the first principles using the generalized-gradient approximation[20] as shown in Fig. 2.

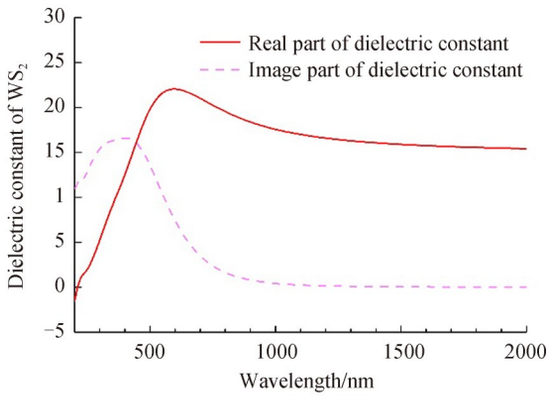

Fig. 2 Simulation results of the dielectric constants of WS_2

To evaluate the RI sensitivity after the tapering and after the addition of WS_2, the transfer matrix method of the multi-layer model[21] is employed to simulate the characteristics of the sensor. The normalized transmission power at the output end of the fiber is given by[7]

$$P_{\text{trans}}=\frac{\int_0^L \mathrm{d}z\int_{\phi_1(z)}^{\phi_2(z)} R_{\text{p}}^{N_{\text{ref}}(\theta,z)}\dfrac{n_1^2\sin\theta\cos\theta}{(1-n_1^2\cos^2\theta)^2}\mathrm{d}\theta}{\int_0^L \mathrm{d}z\int_{\phi_1(z)}^{\phi_2(z)}\dfrac{n_1^2\sin\theta\cos\theta}{(1-n_1^2\cos^2\theta)^2}\mathrm{d}\theta} \tag{1}$$

In the formula, $R_{\text{p}}(\theta,z)$ is the reflectivity of p-polarized incident light and can be calculated by the N-layer matrix method. Φ_1 and Φ_2 are the angle changes caused by the fiber tapering[7]. N_{ref} is the number of reflections experienced by the light in the tapered sensing area (the length of the tapered area is L) and is given by

$$N_{\text{ref}}(\theta,z)=\frac{L}{2\rho(z)\tan(\theta+\Omega)} \tag{2}$$

where $\rho(z)$ is the taper radius varying with distance, and Ω is the taper angle[7].

1.3 Simulation and analysis of fiber optic SPR sensor

The transmission characteristics of the sensor are simulated using the above transmission matrix model. In order to better study the influence of the tapering ratio and the WS_2 film on the SPR phenomenon, the multimode fiber with a core diameter of 600 μm is selected as the substrate of the sensor due to its robust and large contact reaction area[20].

1.3.1 *Effect of taper ratio*

Sensitivity is the main parameter that intuitively describes the performance of the sensor, which can be expressed as follows

$$S=\Delta\lambda/\Delta n \tag{3}$$

where $\Delta\lambda$ is the shift of the resonance wavelength, and Δn is the change of the sensing RI. The sensitivity under different tapering ratios is simulated in order to explore the influence of the tapering ratio on the sensor. The relationship between the sensitivity and the tapering ratio is shown in Fig. 3(a). It can be seen that, as the tapering ratio increases, the sensitivity also gradually increases. However, the increase in the tapering ratio will make the diameter of the fiber smaller, which will reduce the mechanical strength and increase the complexity of subsequent experiments. Therefore, the fiber optic sensor with a tapering ratio of 2 is applied in the following discussion. Corresponding resonance spectra in different RI solutions and sensitivity fitting curves of the sensor with a tapering ratio of 2 are shown in Fig. 3(b). The sensitivity of the tapered fiber SPR sensor is increased by 322.551 nm/RIU compared to that of multimode fiber SPR sensors (the tapering ratio of 1).

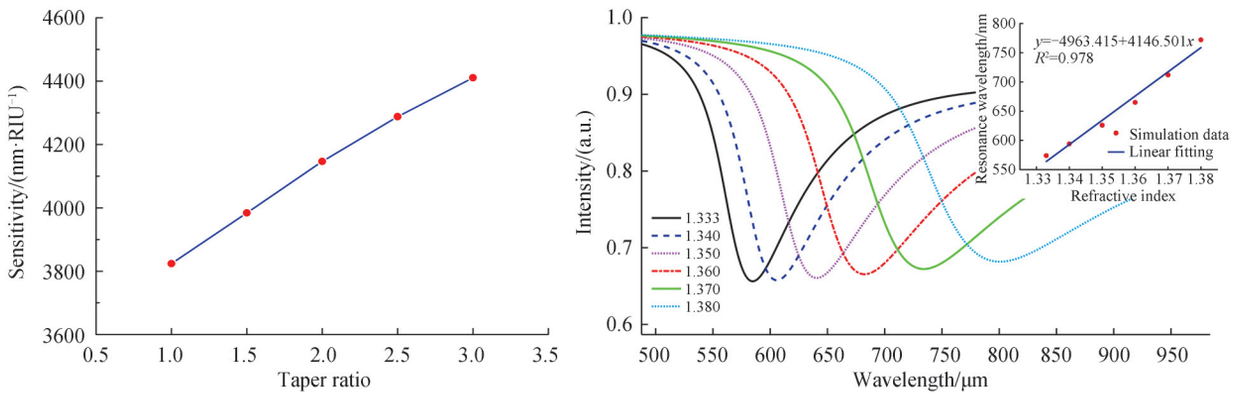

(a) The sensitivity varying with taper ratio　(b) Transmission spectrum with a taper ratio of 3

Fig. 3　The influence of the tapering ratio on the multimode fiber SPR sensor sensitivity

1.3.2　*Effect of the thickness of WS_2*

In the case of a taper ratio of 2, the normalized transmission spectra corresponding to different thicknesses of the WS_2 layer is calculated in Fig. 4(a). As the thickness of the WS_2 layer increases, the sensitivity of the sensor will first increase and then decrease. This is mainly because WS_2 has a high real part in the dielectric constant and a relatively large ratio of complex refractive index[12, 22] which can reduce the energy loss and enhance the evanescent field of the gold film interface. In addition, the evanescent field in the fiber has a larger penetration depth for WS_2 coating than other TDMC materials[21]. In the case of a thinner WS_2 coating, the sensor has a stronger SPR phenomenon, which leads to an enhanced sensitivity. However, as the deposition thickness is further increased, the overlap between the evanescent field and the surface plasma wave of the gold film is reduced, the SPR phenomenon will become weaker, and the sensitivity will also get decreased. Therefore, the interaction between these two effects causes the sensitivity to first increase and then decrease. Fig. 4(b) shows the transmission spectrum and sensitivity fitting curves of the tapered fiber WS_2-Au SPR sensor with WS_2 thickness of 8 nm. Compared to the tapered fiber SPR sensor, the sensitivity is further increased by 155.210 nm/RIU.

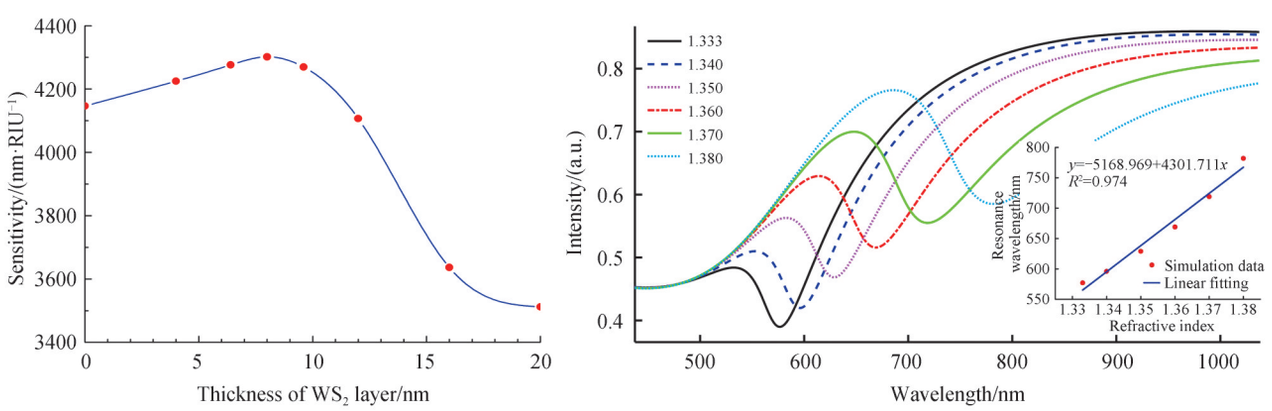

(a) The sensitivity varying with the thickness of WS_2　(b) Transmission spectrum with 8nm thickness of WS_2

Fig. 4　The influence of the WS_2 on the tapered fiber WS_2-Au SPR sensor sensitivity

According to above simulations, the sensor with optimized tapering ratio and WS_2 film thickness can provide the performance improvement to some degree. This theoretically demonstrates the feasibility of the proposed sensor in RI measurement.

2　Experiments

2.1　Fabrication of sensors

Built on numerical simulations, experiments for evaluating and comparing the sensitivities have been

carried out for the multimode fiber SPR sensor, the tapered fiber SPR sensor, the tapered fiber Au-WS_2 SPR sensor and the tapered fiber WS_2-Au SPR sensor. The schematic diagram of the manufacturing process for the tapered fiber WS_2-Au SPR sensor is shown in Fig. 5.

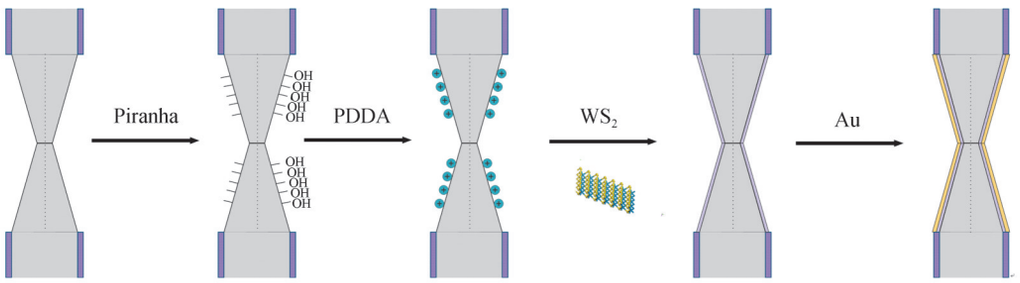

Fig. 5 The manufacturing process of tapered fiber WS_2-Au SPR sensor

2.1.1 *Fabrication of tapered fiber WS_2-Au SPR sensor*

The sensor is fabricated based on a plastic cladded multimode step-index fiber. At first, the non-adiabatic taper with a tapering ratio of 2 is produced via the fusion taper method. The image of tapered fiber is shown in Fig. 6(a). It can be seen that the produced taper has a very good linear transition.

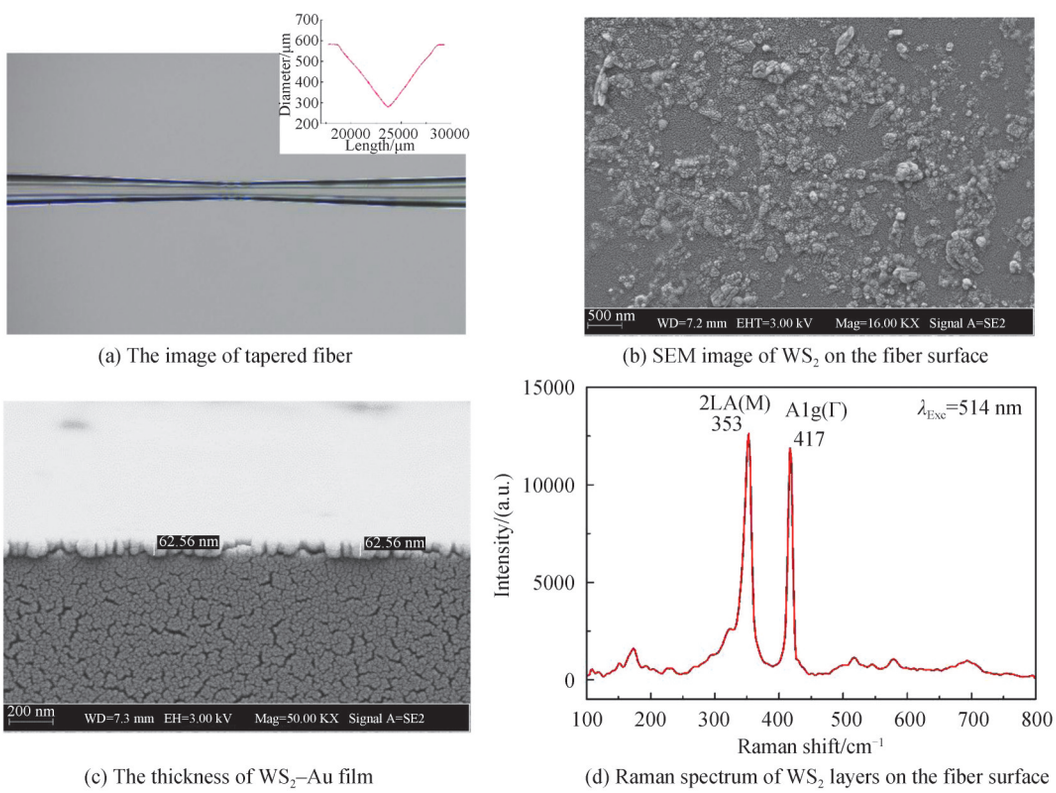

(a) The image of tapered fiber

(b) SEM image of WS_2 on the fiber surface

(c) The thickness of WS_2–Au film

(d) Raman spectrum of WS_2 layers on the fiber surface

Fig. 6 The micrographs of the sensor

Afterwards, WS_2 nanosheets are modified on the surface of the fiber using the electrostatic self-assembly technique[16, 23]. We further place the fiber into a piranha solution to hydroxylate the surface of the fiber and to remove surface impurities. After one hour, the fiber is taken out and the excess piranha solution is cleaned with the deionized water. In the next step, the fiber is immersed in a 1 mg/mL PDDA solution for one hour to positively charge the surface of the fiber. Since the WS_2 nanosheet dispersion is negatively charged, it is modified on the surface of the fiber via the electrostatic adsorption. The fiber from the previous step is fixed in the reaction tube with the ultrasonically treated WS_2 ethanol dispersion solution (1 mg/mL, 100 μL) added. The full evaporation of the dispersion solution means the completion of one deposition cycle. The repetition of

this deposition process can increase the thickness of the WS_2 nanosheets[15]. When the deposition is finished, the sensor is annealed in an environment of 60 ℃ for one hour to improve the stability[24]. The scanning electron microscope (SEM) of WS_2 on the surface of fiber is shown in Fig. 6(b). It can be found that the WS_2 nanosheets with sizes ranging from tens of nanometers to hundreds of nanometers are dispersed on the surface to increase the specific surface area of the fiber, which is beneficial to the improvement of the sensor sensitivity. Finally, a 50 nm thick gold film is sputtered on the modified WS_2 nanosheet fiber using the magnetron sputtering coating technique[25]. The cross-sections of the tapered fiber WS_2-Au SPR sensor is shown in the Fig. 6(c). The thickness of WS_2-Au film on the fiber surface is 62.560 nm. This is basically consistent with the simulated values. It is shown in Fig. 6(d) that Raman scattering spectroscopy is used to characterize the produced sensor. The WS_2 overlayer modified on the surface of the fiber can be regarded as a multilayer film by comparing the intensities of the two Raman mode peaks of 2LA(M) and A1g(Γ)[26].

2.1.2 *Fabrication of other three types of SPR sensor*

The fabrication of the tapered fiber Au-WS_2 SPR sensor is similar to the fabrication of the tapered fiber WS_2-Au SPR sensor. A gold film is sputtered on the surface of the tapered fiber, and then WS_2 nanosheets are coated on the gold film via the electrostatic self-assembly technique.

The tapered fiber is produced by the fusion tapering method, and the 50 nm gold film is sputtered on the tapered fiber and the multimode fiber using the magnetron sputtering coating technique to fabricate the tapered fiber SPR sensor and the 600 μm fiber SPR sensor.

2.2 Experimental setup

The measurement system of the sensor is shown in Fig. 7. The light emitted from the halogen broadband light source (HL-2000, Ocean Optics, Inc. America) is transmitted to the sensor via fiber jumper, and is collected by the spectrometer (HR-4000, Ocean Optics, Inc. America). Additionally, the resonance wavelength is monitored by computer. The transmission spectrum of the sensor for different RI solutions (the solution is made up of deionized water and glycerin with different proportions, and the RI ranges from 1.333 to 1.380) is processed by the computer. 100 data points every 1 s are collected to calculate the standard deviation of the resonance wavelength. The sensor needs to be cleaned three times using the deionized water before the next RI measurement to ensure the accuracy of the detection results. During the experiment, the ambient temperature is maintained at room temperature.

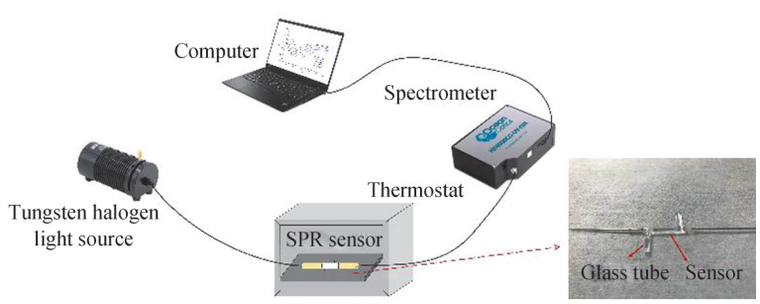

Fig. 7 Experimental measurement system and tapered fiber WS_2-Au SPR sensor

3 Results and discussions

3.1 Sensitization effect of tapered fiber

The transmission spectra of the tapered fiber SPR sensor and the 600 μm fiber SPR sensor under different RI solutions are shown in the Fig. 8. The Empirical Mode Decomposition (EMD) technology[27] is used for noise reduction preprocessing and the polynomial fitting method[9] is used to demodulate the resonance wavelength. When the RI change is 0.047 RIU, the resonance wavelength of the tapered fiber SPR sensor is red-shifted by 101.457 nm, while the resonance wavelength of the 600 μm fiber SPR sensor is only red-shifted by 87.420 nm. Fig. 9 shows the linear fitting curves of the performance for the two sensors. The sensitivity of the tapered fiber SPR sensor is 2 126.536 nm/RIU, which is 15.5% higher than the sensitivity of the 600 μm fiber SPR sensor. Compared to simulation results, the enhancement in the sensitivity is relatively small. On the

one hand, it is difficult to ensure the symmetry of the tapered fiber during the fabrication process. On the other hand, the absorption medium of the sensor is only the gold film. A considerable portion of the evanescent field energy gets lost and is not coupled with surface plasma waves[28].

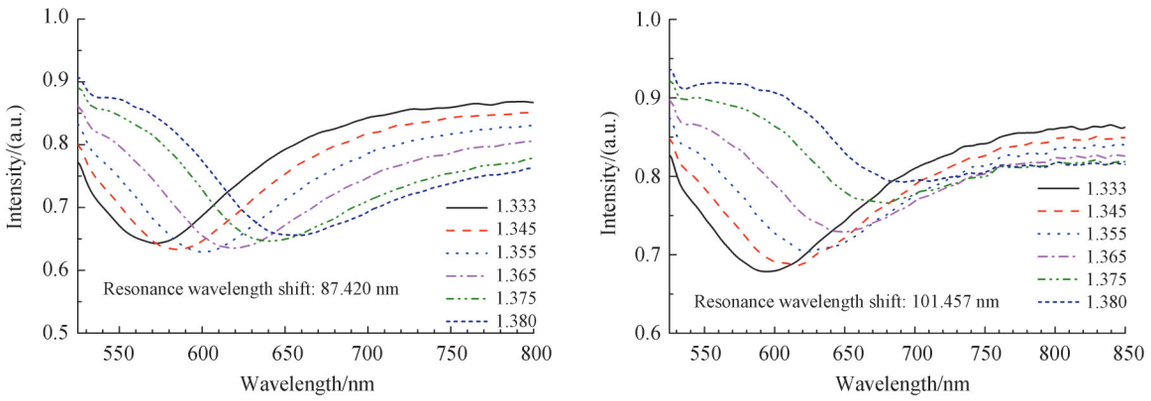

(a) 600 μm fiber SPR sensor (b) Tapered fiber SPR sensor

Fig. 8 The transmission spectrum of sensors

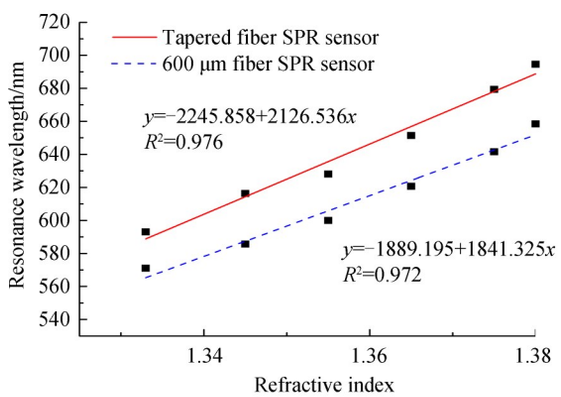

Fig. 9 The RI linear fitting curve of fiber optic SPR sensor without and with taper

3.2 Sensitization effect of WS_2 film

In order to evaluate the effect of WS_2 on the sensor, the sensitivity between the conventional coating method (first sputtering gold film, then coating WS_2) and the proposed coating method (first coating WS_2, then sputtering Au) is compared.

3.2.1 *The structure of Au-WS_2*

To ensure the repeatability, each group of experiments has been repeated five times. The influence of WS_2 on the sensitivity of the sensor is plotted in Fig. 10(a). It is shown that the average RI sensitivity increases significantly from 0 to 3 cycles, and then gradually decreases. The resonance wavelength shows a significant red shift. Fig.10(b) is the transmission spectrum of a sensor after three cycles of deposition in one of the deposition experiments. It can be seen that the sensitivity of the sensor is improved to 2 769.979 nm/RIU, which is 30.3% higher than that of the tapered fiber SPR sensor without WS_2 coating.

The unique photoelectric characteristic of WS_2 is the main reason for the enhancement in the sensitivity of the sensor. The high quantum conversion efficiency of WS_2 nanosheets can stimulate more electrons to be transferred from WS_2 to the gold film[29], and the transfer of electrons can enhance the surface electric field to improve the coupling efficiency of the SPR sensor.

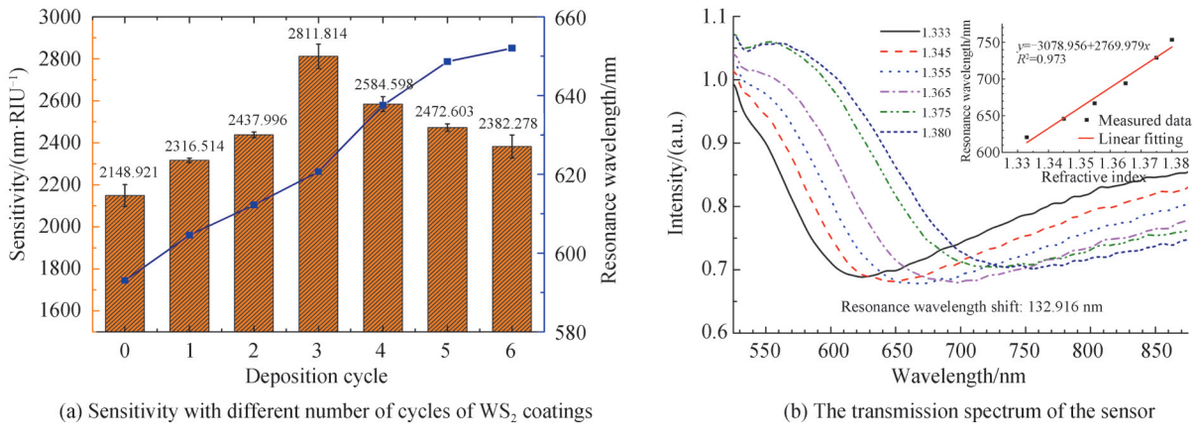

(a) Sensitivity with different number of cycles of WS_2 coatings (b) The transmission spectrum of the sensor

Fig. 10 The characteristic of the tapered fiber Au-WS_2 SPR sensor

3.2.2 *The structure of WS_2-Au*

The measurement process of the RI sensitivity for the tapered fiber WS_2-Au SPR sensor is similar as that of the above three sensors. The transmission spectrum of the sensor coated with 4 cycles of WS_2 nanosheets is shown in Fig. 11(b). When the RI change is 0.047 RIU, the resonance wavelength of the sensor is red-shifted by 186.810 nm.

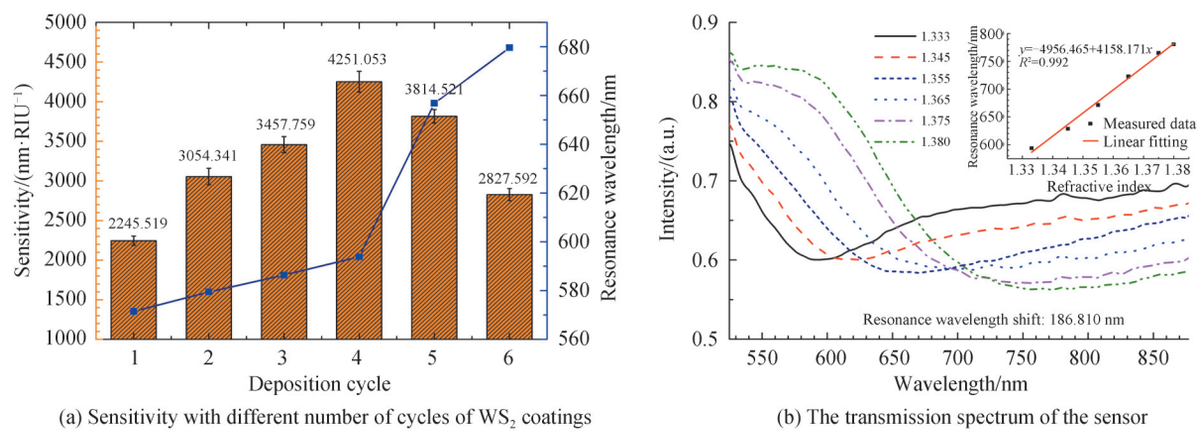

(a) Sensitivity with different number of cycles of WS_2 coatings (b) The transmission spectrum of the sensor

Fig. 11 The characteristic of the tapered fiber WS_2-Au SPR sensor

Similarly, the effect of different WS_2 deposition cycles is studied in Fig. 11(a), and a similar conclusion as the Au-WS_2 sensor can be obtained. After coating four cycles of WS_2, the sensitivity of the WS_2-Au sensor can reach 4 158.171 nm/RIU, which is 50.1% higher than that of the Au-WS_2 sensor. It is seen that the sensor with WS_2 coated between the fiber and the gold film provides a better sensitivity than sensor with WS_2 coated on the surface of the gold film. However, the spectral broadening caused by the radiation damping of WS_2 is inevitable[30].

3.3 Discussions

According to the above results, coating WS_2 has a significant enhancement effect on the sensitivity of the tapered fiber SPR sensor in the Fig. 12(a). This is mainly attributed to photoelectric properties of WS_2. The fiber tapering can enhance the strength of the evanescent field, but some rays do not meet the total reflection condition, and are not coupled with the plasma wave. When only the gold film is coated, it is not enough for the sensor to stimulate a strong SPR effect. When WS_2 is coated between the fiber and the gold film, the good photon absorption characteristics of WS_2 can effectively increase the absorption of light energy, and can thereby enhance the energy coupling. In addition, high quantum efficiency and high complex RI ratio of WS_2 can reduce the energy loss during the electron transfer process and can enhance the electric field intensity on the surface. Therefore, good photon absorption characteristics and high quantum conversion efficiency of the WS_2

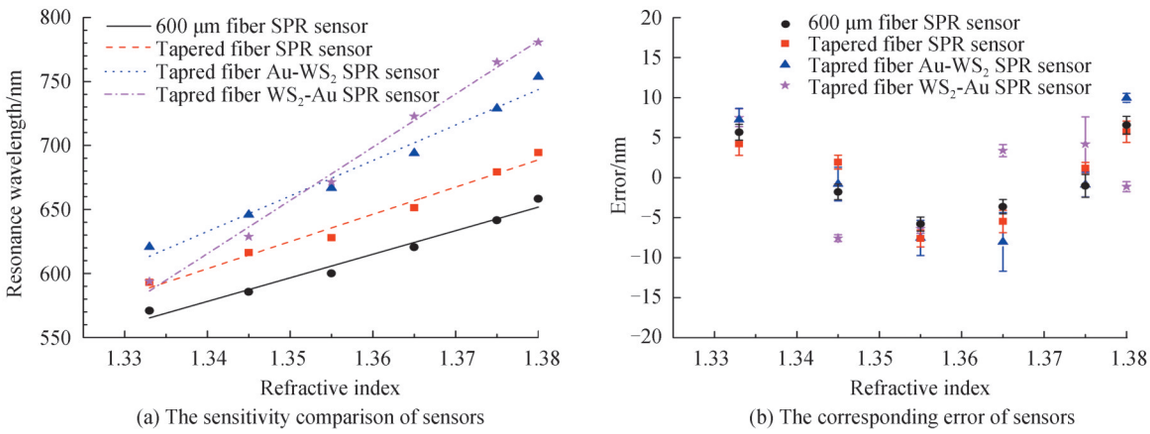

(a) The sensitivity comparison of sensors (b) The corresponding error of sensors

Fig. 12 The characteristic of fiber optic SPR sensors with four different structures

nanosheets between the fiber surface and the gold film can greatly improve the RI sensitivity of the sensor and can make the sensor more sensitive to changes in the external environment. The coating of WS_2 nanosheets on the surface of the gold film will only increase the photon utilization rate of the sensor system, and thus the tapered fiber Au-WS_2 SPR sensor shows a relatively small increase in the sensitivity compared to the sensor with the WS_2-Au structure. It is worth mentioning that the WS_2 coated on the surface of the gold film is easier to fall off during the experiment than the WS_2 coated on the inner side. Therefore, the proposed sensor has better sensitivity and reliability.

From above analyses, the good linear relationship between the resonance wavelength and the sensing RI demonstrates that the sensing RI change can be well detected through observing the shift in the resonance wavelength. The proposed tapered fiber WS_2-Au structure sensor is compared with other reported SPR sensors in terms of structure complexity of sensors, as shown in Table 1. It is seen that the proposed sensor has a relatively simple structure to provide a significant sensitivity enhancement in the refractive index range of 1.333~1.380 (corresponding to the biochemical sensing window).

Table 1 Comparison of sensors with different structures

Sensor structure	RI range	Sensitivity	Method	References
Au-polydopamine-$MoSe_2$@AuNPS	1.333~1.358	5 117.59 nm/RIU	Experiment	[9]
Ag-black phosphorene-graphene	1.330~1.390	4 050 nm/RIU	Simulation	[22]
Au-WS_2 (prism)	1.333~1.360	2 459.3 nm/RIU	Experiment	[15]
Au-$MoSe_2$ (multimode fiber)	1.333~1.358	2 793.36 nm/RIU	Experiment	[18]
Au-WS_2 (tapered fiber)	1.333~1.380	2 769.979 nm/RIU	Experiment	Proposed scheme
WS_2-Au (tapered fiber)	1.333~1.380	4 158.171 nm/RIU	Experiment	Proposed scheme

4 Conclusion

In this paper, a tapered fiber SPR sensor with the WS_2-Au structure is proposed. The influence of tapering and WS_2 nanomaterial on the fiber optic SPR sensing system is investigated. The theoretical feasibility of the sensor is proved using the transfer matrix method. WS_2 is modified on the fiber surface via the electrostatic self-assembly technique, and then the gold film is sputtered to fabricate the sensor. The experimental RI sensitivity of the proposed sensor can reach 4 158.171 nm/RIU, which is 125.8% higher than that of the 600 μm fiber SPR sensor. Experimental results show a good agreement with the numerical simulations. It is demonstrated that the introduction of the WS_2 layer can improve the sensitivity of the fiber optic SPR sensor and enhance the reliability of the sensor. In summary, the developed sensor can provide a high-sensitivity, low-cost, simple and environment-friendly platform for the biochemical detection.

References

[1] SEMWAL V, SHRIVASTAV A M, VERMA R, et al. Surface plasmon resonance based fiber optic ethanol sensor using

layers of silver/silicon/hydrogel entrapped with ADH/NAD[J]. Sensors and Actuators B: Chemical, 2016, 230: 485-492.
[2] KAUSHIK S, TIWARI U K, DEEP A, et al. Two-dimensional transition metal dichalcogenides assisted biofunctionalized optical fiber SPR biosensor for efficient and rapid detection of bovine serum albumin[J]. Scientific Reports, 2019, 9: 1-11.
[3] PASQUARDINI L, CENNAMO N, MALLEO G, et al. A surface plasmon resonance plastic optical fiber biosensor for the detection of Pancreatic amylase in surgically-placed drain effluent[J]. Sensors, 2021, 21(10): 3443.
[4] HOMOLA J, YEE S S, GAUGLITZ G. Surface plasmon resonance sensors: review[J]. Sensors and actuators B: Chemical, 1999, 54(1-2): 3-15.
[5] ZHANG Z, LIU K, JIANG J F, et al. Refractometric sensitivity enhancement of weakly tilted fiber Bragg grating integrated with black phosphorus[J]. Nanomaterials, 2020, 10(7): 1423-1432.
[6] VERMA R K, SHARMA A K, GUPTA B D, Modeling of tapered fiber-optic surface plasmon resonance sensor with enhanced sensitivity[J]. IEEE Photonics Technology Letters, 2007, 19(22): 1786-1788.
[7] VERMA R K, SHARMA A K, GUPTA B D. Surface plasmon resonance based tapered fiber optic sensor with different taper profiles[J]. Optics Communications, 2008, 281(6): 1486-1491.
[8] VIVEK S, GUPTA B D. Experimental studies on the sensitivity of the propagating and localized surface plasmon resonance-based tapered fiber optic refractive index sensors[J]. Applied Optics, 2008, 58(15): 4149-4156.
[9] LIU K, ZHANG J H, JIANG J F, et al. Multi-layer optical fiber surface plasmon resonance biosensor based on a sandwich structure of polydopamine-$MoSe_2$@Au nanoparticles-polydopamine[J]. Biomedical Optics Express, 2020, 11(12): 6840-6851.
[10] ROLI V, GUPTA B D, JHA R. Sensitivity enhancement of a surface plasmon resonance based biomolecules sensor using graphene and silicon layers[J]. Sensors and Actuators B: Chemical, 2011, 160(1): 623-631.
[11] MESHGINQALAM B, AHMADI M T, ISMAIL R, et al. Graphene/graphene oxide-based ultrasensitive surface plasmon resonance biosensor[J]. Plasmonics, 2017, 12(6): 1991-1997.
[12] WU L, CHU H S, KOH W S, et al. Highly sensitive graphene biosensors based on surface plasmon resonance[J]. Optics Express, 2010, 18(14): 14395-14400.
[13] WU L M, GUO J, WANG Q K, et al. Sensitivity enhancement by using few-layer black phosphorus-graphene/TMDCs heterostructure in surface plasmon resonance biochemical sensor[J]. Sensors and Actuators B: Chemical, 2017, 249: 542-548.
[14] OUYANG Q L, ZENG S W, JIANG L, et al. Sensitivity enhancement of transition metal dichalcogenides/silicon nanostructure-based surface plasmon resonance biosensor[J]. Scientific Reports, 2016, 6(1): 1-13.
[15] WANG H, ZHANG H, DONG J L, et al. Sensitivity-enhanced surface plasmon resonance sensor utilizing a tungsten disulfide (WS_2) nanosheets overlayer[J]. Photonics Research, 2018, 6(6): 485-491.
[16] SONG H, WANG Q, ZHAO W. A novel SPR sensor sensitivity-enhancing method for immunoassay by inserting MoS_2 nanosheets between metal film and fiber[J]. Optics and Lasers in Engineering, 2020, 132: 106135.
[17] MA J Y, LIU K, JIANG J F, et al. Theoretical and experimental investigation of an all-fiber waveguide coupled surface plasmon resonance sensor with Au-ZnO-Au sandwich structure[J]. IEEE Access, 2019, 7: 169961-169968.
[18] LIU K, ZHANG J H, JIANG J F, et al. $MoSe_2$-Au based sensitivity enhanced optical fiber surface plasmon resonance biosensor for detection of goat-anti-rabbit IgG[J]. IEEE Access, 2019, 8: 660-668.
[19] SARIKA S, SHARMA N. K, SAJAL V. Theoretical study of surface plasmon resonance-based fiber optic sensor utilizing cobalt and nickel films[J]. Brazilian Journal of Physics, 2016, 46(3): 288-293.
[20] MA J Y, LIU K, JIANG J F, et al. All optic-fiber coupled plasmon waveguide resonance sensor using ZrS_2 based dielectric layer[J]. Optics Express, 2020, 28(8): 11280-11289.
[21] BAHAR M, BARVESTANI J. Performance enhancement of SPR biosensor based on phosphorene and transition metal dichalcogenides for sensing DNA hybridization[J]. IEEE Sensors Journal, 2018, 18(18): 7537-7543.
[22] RAHMAN M S, ANOWER M S, ABDULRAZAK L F. Utilization of a phosphorene-graphene/TMDC heterostructure in a surface plasmon resonance-based fiber optic biosensor[J]. Photonics and Nanostructures-Fundamentals and Applications, 2019, 35: 100711.
[23] XUE T, QI K, HU C. Novel SPR sensing platform based on superstructure MoS2 nanosheets for ultrasensitive detection of mercury ion[J]. Sensors and Actuators B: Chemical, 2019, 284: 589-594.
[24] CHANG P X, LIU K, JIANG J F, et al. Performance enhancement of the surface plasmon resonance sensor through the annealing process[J]. IEEE Access, 2020, 8: 33990-33997.
[25] WANG T, ZHANG M J, LIU K, et al. The effect of the TiO_2 film on the performance of the optical fiber SPR sensor[J]. Optics Communications, 2020, 448: 93-97.
[26] BERKDEMIR, GUTIERREZ H R, BOTELLO-MENDEZ A R, et al. Identification of individual and few layers of WS_2 using Raman spectroscopy[J]. Scientific Reports, 2013, 3(1): 1-8.
[27] WANG T, LIU T G, LIU K, et al. An EMD-based filtering algorithm for the fiber-optic SPR sensor[J]. IEEE

Photonics Journal, 2016, 8(3): 1-8.
[28] RAHMAN M S, HASAN M R, RIKTA K A, et al. A novel graphene coated surface plasmon resonance biosensor with tungsten disulfide (WS_2) for sensing DNA hybridization[J]. Optical Materials, 2018, 75: 567-573.
[29] ALAGDAR M, YOUSIF B, AREED N F, et al. Improved the quality factor and sensitivity of a surface plasmon resonance sensor with transition metal dichalcogenide 2D nanomaterials[J]. Journal of Nanoparticle Research, 2018, 22(7): 1-13.
[30] DASTMALCHI B, TASSIN P, KOSCHNY T, et al. A new perspective on plasmonics: confinement and propagation length of surface plasmons for different materials and geometries[J]. Advanced Optical Materials, 2016, 4(1): 177-184.

Tungsten Disulfide Modified Tapered Fiber Optic Surface Plasmon Resonance Sensor with Enhanced Sensitivity

ZHANG Wenlin, LIU Kun, JIANG Junfeng, XU Tianhua, WANG Shuang, ZHANG Zhao, JING Jianying, MA Jinying, LIU Tiegen

(*Key Laboratory of Optoelectronics Information Technology, Ministry of Education, School of Precision Instruments and Optoelectronics Engineering, Tianjin University, Tianjin* 300072, *China*)

Abstract: Fiber optic SPR sensors have wide application prospects in the field of biosensing due to the advantages of label-free, fast response in real-time, and good biocompatibility. Traditional multimode fiber optic SPR sensors are limited by low sensitivity, which leads to their insufficient performance in the detection of low-concentration analytes. Therefore, improving the sensitivity of fiber optic SPR sensors and applying them to trace detection of biomolecules have received increasing attention from researchers. There are two main ways to improve sensitivity. One is to increase the strength of the evanescent field by changing the structure of fiber (e.g. U-shaped, D-shaped, tapered, etc.), and the other is to use the excellent photoelectric properties of new materials (e.g. high refractive index oxides, ceramic materials, two-dimensional materials, etc.) to improve the sensitivity of the sensor. Similar to graphene, Transition Metal Dichalcogenides (TMDCs) have also attracted much attention. Among them, Tungsten disulfide (WS_2) shows many unique optoelectronic properties such as high complex RI ratio (the ratio of the real part to the imaginary part of the RI), direct band gap and large surface-to-volume ratio. It is shown that the application potential of WS_2 in SPR sensors. However, there are relatively few experimental studies of WS_2 in SPR sensors, and they mainly focus on prism-based SPR sensors.Based on the above-mentioned methods, the sensitivity of the fiber optic SPR sensor is improved by combining the tapering of the fiber and the coating of WS_2 nanomaterials. In this paper, a tapered fiber optic SPR sensor based on the structure of WS_2-Au is proposed. The relationship between the dielectric constant of WS_2 and the wavelength is obtained by the first principles using the generalized-gradient approximation. The effects of taper ratio and the thickness of WS_2 on the sensitivity of sensors are studied through theoretical simulations used the transfer matrix method. Then, four kinds of sensors (600 μm fiber SPR sensor, tapered fiber SPR sensor, tapered fiber Au-WS_2 SPR sensor and tapered fiber WS_2-Au SPR sensor) are manufactured. Among them, the WS_2 nanosheets are modified on the fiber surface using electrostatic self-assembly technology, and the Au film is obtained by vacuum magnetron sputtering coating technology. An experimental setup is built to measure their Refractive Index (RI) sensitivity. The experimental RI sensitivity of the proposed tapered fiber WS_2-Au SPR sensor can reach 4 158.171 nm/RIU, which is 125.8% higher than that of the multimode fiber SPR sensor and 50.1% higher than that of the tapered fiber Au-WS_2 SPR sensor. Experimental results show a good agreement with the numerical simulations. It is demonstrated that the introduction of the WS_2 layer can improve the sensitivity of the fiber optic SPR sensor and enhance the reliability of the sensor. In summary, the developed sensor can provide a high-sensitivity, low-cost, simple and environment-friendly platform for the biochemical detection.

Key words: Surface plasmon resonance; Tapered fiber; Sensitivity; Tungsten disulfide; Sensor
OCIS Codes: 060.0060; 060.2310; 060.2370